

Model Bicontinuous Microemulsions in Ternary Homopolymer/Block Copolymer Blends

Marc A. Hillmyer,^{*,†} Wayne W. Maurer,^{†,§} Timothy P. Lodge,^{†,§} and Frank S. Bates^{*,§}*Department of Chemistry and Department of Chemical Engineering and Materials Science, University of Minnesota, Minneapolis, Minnesota 55455*

Kristoffer Almdal

*Department of Solid State Physics, Risø National Laboratory, DK-4000 Roskilde, Denmark**Received: January 6, 1999; In Final Form: April 8, 1999*

We have identified a channel of bicontinuous microemulsion in three chemically distinct homopolymer/homopolymer/block copolymer (A/B/A–B) ternary blends. Experiments were conducted along the isopleth, defined by equal volumes of homopolymer and varying amounts of block copolymer, as a function of temperature. A symmetric condition was achieved through the use of homopolymers with matched degrees of polymerization ($N_A \approx N_B = N_H$) and compositionally symmetric diblock copolymers ($f \approx 0.5$) where $\alpha \equiv N_{AB}/N_H \approx 0.2$. We explored PE–PEP/PE/PEP (EP), PEE–PDMS/PEE/PDMS (EED), and PE–PEO/PE/PEO (EO) ternary systems differing in molecular weight by nearly 2 orders of magnitude. Using a combination of small-angle neutron scattering (SANS), rheology, and cloud point measurements, we mapped the phase diagram along the isopleth for each of these systems. On the block-copolymer-rich side of the phase diagrams, a line of lamellar-disorder transitions was observed. On the homopolymer-rich side of the phase diagrams, a line of transitions separating one-phase and phase-separated regions was found. A narrow channel of bicontinuous microemulsion separates these two regimes in all three systems. This bicontinuous microemulsion phase is similar to the analogous bicontinuous phases found in oil/water/surfactant mixtures. We have demonstrated that there is a common region in phase space over which the bicontinuous microemulsion is stable in these polymeric systems and that the general phase behavior is independent of polymer molecular weight. The low molecular weight of the EO system is ideal for fundamental phase behavior studies in polymeric blends, since the kinetic limitations that plague high-molecular-weight mixtures are avoided. Furthermore, the EO system utilizes polyethylene–poly(ethylene oxide) block copolymers that are chemically very similar to well-known nonionic surfactants, and thus, connections to surfactancy can readily be made.

Introduction

Water and oil are not miscible. The water/oil interface in a macroscopically phase-separated mixture can be stabilized by the addition of amphiphilic molecules such as surfactants. As the name implies, these surface-active agents can reside at the water/oil interface and significantly reduce the interfacial tension between the two domains. At certain compositions oil, water, and a suitable surfactant can form a thermodynamically stable structure referred to as a microemulsion.¹ Microemulsions can be categorized into three main types: oil-in-water (the most common), water-in-oil, and bicontinuous. The common feature of these microemulsions is the presence of a surfactant-saturated interface between the oil and water domains. The oil-in-water and water-in-oil microemulsions consist of droplets of one phase dispersed in the other continuous phase and are referred to as droplet microemulsions. Bicontinuous microemulsions, on the other hand, are observed in mixtures that contain roughly equal amounts of oil and water and have a fundamentally different morphology. Direct visualization of the bicontinuous morphology, a spongelike structure, has been accomplished using freeze fracture electron microscopy.²

Microemulsions are “complex fluids”^{3,4} that have found many technological applications including detergency, enhanced oil recovery, and pharmaceuticals. In addition, a variety of chemical reactions can be performed in microemulsions such as nanoparticle formation, polymerizations,⁵ and electrochemical reactions. These reactions, as well as other technical applications of microemulsions, have been reviewed recently.⁶ In part because of their usefulness there have been many theoretical and experimental studies on the properties of microemulsions,⁷ particularly the bicontinuous variety. These disordered structures resemble the isotropic L_3 phase observed in surfactant/water mixtures.⁸ However, in typical surfactant systems such as nonionic surfactant/water/oil mixtures the region of phase space over which the bicontinuous microemulsion phase is stable is quite small.

Consider a 50/50 mixture of oil (A) and water (B) containing variable amounts of nonionic surfactant (AB; see Figure 1b). At low surfactant concentrations (γ), there are not enough amphiphilic molecules to stabilize the oil/water interface, and the mixture phase-separates into oil-rich and water-rich phases. At high surfactant concentrations a lamellar liquid crystalline phase, a viscous anisotropic structure consisting of layers of oil and water separated by the amphiphile, is formed. The crossover in surfactant concentration between these two limiting

* To whom correspondence should be addressed.

† Department of Chemistry.

‡ Current address: 3M Company, 3M Center, St. Paul, MN 55144.

§ Department of Chemical Engineering and Materials Science.

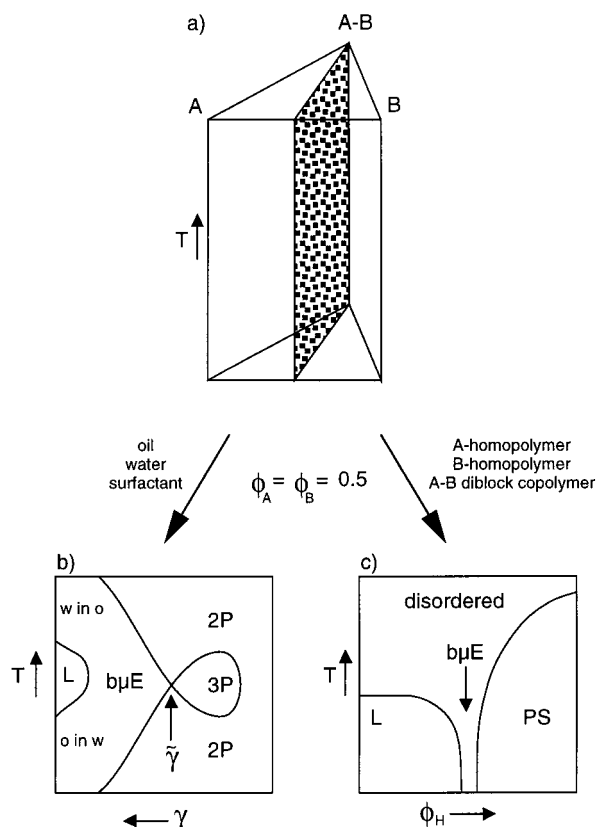


Figure 1. (a) Phase prism for a three-component system. (b) "Fish-cut" isopleth for a general oil/water/nonionic surfactant mixture at equal volumes of oil and water. (c) "Fish-cut" isopleth for an A/B/AB homopolymer-block copolymer mixture. γ = surfactant concentration, Φ_H = concentration of homopolymer in the ternary blend, b μ E = bicontinuous microemulsion, L = lamellar phase, 2P = two-phase, 3P = three-phase, PS = phase-separated region (2P or 3P).

behaviors depends on the type of surfactant used but is typically between 10 and 30%. It is between these two extremes that microemulsions are stable. However, in the case of nonionic surfactants the temperature dependence of the surfactant solubility further restricts the region in the phase diagram over which the bicontinuous microemulsion phase is stable. At low surfactant concentrations two macroscopic phases exist and the amphiphile is mainly dissolved in the water phase at ambient temperature. However, as the temperature is increased, the amphiphile prefers the oil phase and at high temperatures becomes dissolved mainly in the oil phase. As the concentration of the amphiphile is further increased, a three-phase regime intervenes, composed of an oil-rich phase, a water-rich phase, and a microemulsion phase. At intermediate temperature the surfactant is only slightly soluble in both the oil and the water phases and can only be accommodated at the oil/water interface, giving rise to a microemulsion phase. As the surfactant concentration increases, the three-phase temperature window at first increases in size and then decreases until it eventually disappears. At this point in surfactant concentration $\tilde{\gamma}$, small increases in surfactant concentration lead to two phases at low temperature, two phases at high temperature, and at intermediate temperatures a homogeneous, one-phase solution of all three components. Microemulsions are stable in this one-phase region; however, the change in solubility of the amphiphile with temperature leads to further restrictions in phase space for the bicontinuous microemulsion. Oil-in-water microemulsions exist at low temperature and water-in-oil microemulsions at high temperature.

The above description of the complex thermodynamics of symmetric water/oil/surfactant mixtures can be represented by a phase diagram that depends on temperature and surfactant concentration. The diagram resembles a fish⁹ and is referred to as the isopleth or "fish-cut" (Figure 1b) of the ternary phase prism (Figure 1a). The point in the phase diagram where the minimum amount of amphiphile necessary to stabilize a homogeneous microemulsion ($\tilde{\gamma}$) depends on the "strength" of the amphiphile. The stronger the amphiphile the lower $\tilde{\gamma}$. The temperature range over which microemulsions are stable also depends on the amphiphile but can be tuned to some degree by the addition of cosolvents, the nature of the oil, or the salinity of the aqueous phase. Because of the variety in real systems, there is no universal amphiphile that can stabilize microemulsions over a prescribed temperature range for all possible combinations of oil and water. This fact has led to the design of new amphiphiles for specific applications where microemulsions are required. Comparison of chemically different systems is thwarted by the inability to make comparisons over similar temperature ranges.

Three-component mixtures containing two immiscible liquids and an amphiphile can be extended to other systems that do not necessarily contain water as one of the components. Because of the peculiar change in "philicity" of nonionic amphiphiles in the presence of water, three component systems that do not contain water are of interest. A mixture of immiscible polymers in the presence of a suitable block copolymer is such a system. Block copolymers have been used to stabilize mixtures of immiscible pairs of polymers,¹⁰ since AB block copolymers can act much like surfactants by accumulating at the interface between phases of the two homopolymers A and B.

As part of our general interest in block copolymer phase behavior, we have investigated three-component mixtures of model homopolymers and block copolymers in a polyolefin system and reported on the critical scattering¹¹ and phase morphology¹² of these mixtures. The isopleth in the ternary phase prism (analogous to the "fish-cut" for oil/water/surfactant systems) was determined and is shown schematically in Figure 1c. Although there are fundamental differences between the two isopleths in the o/w/s and the A/B/AB systems, there are certain similarities. At low AB concentrations the A and B homopolymers form a two-phase region at low temperatures. However, unlike the o/w/s system, increasing temperature leads to single homogeneous phase, reflecting homopolymer blend upper critical solution temperature behavior. At high block copolymer concentrations an ordered lamellar phase and a disordered phase are observed at low and high temperatures, respectively. This behavior resembles the well-documented order-disorder phenomena observed in pure block copolymers.¹³ It is between these two extremes that a channel of bicontinuous microemulsion was identified by small-angle scattering and transmission electron microscopy experiments.¹²

Encouraged by the discovery of a bicontinuous microemulsion phase in a high-molecular-weight polyolefin system, we became interested in the universality of this behavior, with particular emphasis on the effect of composition fluctuations, and the dynamics of these in ternary polymer mixtures.¹⁴ The phenomenological connections between the phase behavior of block copolymers and low-molecular-weight surfactant solutions have resulted in an experimental effort designed to provide a more complete understanding of the similarities and differences in these two systems.¹⁵ To this end, we synthesized a set of low-molecular-weight amphiphilic block copolymers consisting of an alkane segment and a poly(ethylene oxide) segment.¹⁶ These

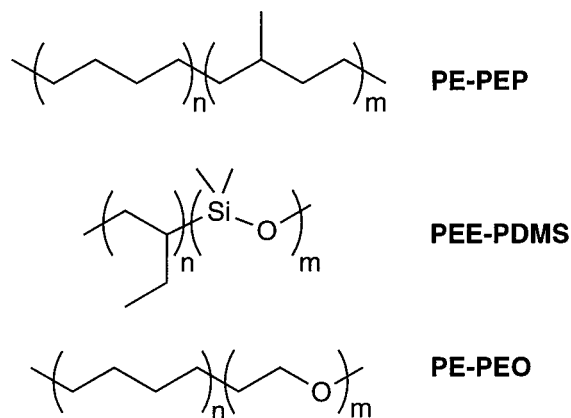


Figure 2. Chemical structures of block copolymers used in this study. The corresponding homopolymers are chemically identical to the respective segments in the block copolymers.

materials are chemically very similar to the well-known nonionic surfactants. We studied the phase behavior of these block copolymers in the neat state and as aqueous dispersions.¹⁷ With one chemical system, we were able to continuously study both the thermotropic and lyotropic (solution) phase behavior. A logical extension of our work with these amphiphilic block copolymers in the neat state and in the presence of water is the study of ternary mixtures with the corresponding homopolymers. In addition to the low-molecular-weight poly(ethylene oxide) based system, we have prepared another chemically distinct system that is intermediate in molecular weight between the polyolefin and the poly(ethylene oxide) block copolymers. This poly(dimethylsiloxane)–polyethylethylene system serves as a natural connection between the two molecular weight extremes.¹⁸

In this paper we compare the ternary blend phase behavior for the three chemically distinct systems shown in Figure 2. Using a combination of small-angle neutron scattering (SANS), cloud point measurements, and rheology, we have mapped the phase behavior of 50/50 mixtures of the A and B homopolymers with varying amounts of block copolymer (isopleth or “fish cut” of the phase prism). In all three systems, we have located a channel of bicontinuous microemulsion.

Experimental Section

Materials. The polyolefin block copolymers described here are the identical materials described in ref 13. Synthesis of the polyethylene–poly(ethylene oxide) block copolymer used in this study was described in ref 16 where it is referred to as EO-1. The low-molecular-weight polyethylene sample was prepared by anionic polymerization of butadiene-*d*₄ followed by catalytic saturation with D₂. The dimethoxy PEO homopolymer was obtained from Fluka (81313, analysis 307448/1 993), dissolved in benzene, and freeze-dried at room temperature under vacuum ($\sim 10^{-3}$ Torr). The sample was then heated under vacuum at 60 °C for 30 min, cooled to room temperature (RT), and blanketed with high-purity argon. The sample was stored in a dark-brown bottle under nitrogen. The polyethylethylene–poly(dimethylsiloxane) block copolymer was prepared by sequential anionic polymerization as described in ref 18.

The PEE homopolymer was synthesized by anionic polymerization of butadiene in THF solution at temperatures between -53 and -14 °C; *sec*-butyllithium was used as initiator. The resultant polybutadiene was saturated with D₂ in cyclohexane solution using a Pd/CaCO₃ catalyst. The molar mass of the PEE was determined through NMR spectroscopy of the diene

polymer (Table 1). The PDMS homopolymer was prepared in THF solution. *sec*-Butyllithium initiator was added to THF at -60 to -40 °C. Hexamethylcyclotrisiloxane was added at -60 to -30 °C, and the solution was allowed to warm to room temperature. The polymerization was terminated by addition of trimethylchlorosilane. The molar mass of the PDMS–homopolymer was determined through NMR spectroscopy (Table 1).

The densities of PEE, PDMS, and PEE–PDMS were measured at room temperature using a density gradient column. The amorphous densities of PEO, PE, and PE–PEO are difficult to obtain using this technique because of interference from crystallinity and solubility in the density gradient medium. Therefore, the densities of the low-molecular-weight PE and PEO homopolymers were calculated for each of these materials at 140 °C using the high-molecular-weight densities¹⁹ and correcting for temperature, molecular weight, and deuterium substitution.²⁰ The density of the PE–PEO block copolymer was determined using additivity of the calculated molar volumes of the two component blocks ([molar volume of PE + molar volume of PEO]/molar mass of the block copolymer).²¹ From these measurements the number of repeat units in a common segment volume was calculated. These values are given in Table 1.

Blend Preparation. The high-molecular-weight polyolefin ternary blends were prepared in a similar manner as the blends described in ref 11. The low-molecular-weight PE/PEO/PE–PEO blends and the PEE/PDMS/PEE–PDMS blends were easily prepared in the melt state because of the low viscosity of the polymers at moderate temperatures. For the cloud point determinations the liquid homopolymers were transferred by syringe to a pretared ampule. Small portions of the corresponding block copolymer were added to the ampule containing a 50/50 (v/v) mixture of the homopolymers. A small magnetic stir bar was placed in the mixture, and the ampule was flame-sealed under vacuum after thorough degassing. The blends were then heated and stirred until a one-phase solution was obtained. At RT most of the samples were phase-separated, so it was difficult to accurately transfer a premixed blend into a cell suitable for SANS studies. Therefore, we prepared blends for SANS measurements directly in the cells. The cells used for the SANS studies were constructed using two quartz disks that were sealed around the edges with a melted quartz rod. The disks were separated by a precision-machined stainless steel spacer. The stainless steel spacer (0.1022 ± 0.0005 cm) was removed after a small amount of the molten quartz rod was applied to the gap between the disks as a support. After the spacer was removed, the rest of the cell was sealed with quartz. The as-fabricated cells were cut along one edge to provide access to the cell interior. The polymer samples were added to these cells under nitrogen using a syringe. A small fleck of iron wire was added to the cell as a magnetic stir bar. The cells were sealed under nitrogen using a commercial epoxy. The blends were homogenized by heating the cells on a hot plate with a magnetic stirrer prior to SANS analysis.

Small-Angle Neutron Scattering. SANS measurements were performed at the National Institute of Standards and Technology (NIST) in Gaithersburg, Maryland on the NIST/Exxon/University of Minnesota 30 m instrument using $\lambda = 7$ Å wavelength neutrons ($\Delta\lambda/\lambda = 0.11$) and at Risø National Laboratory in Roskilde, Denmark with 5.6 Å neutrons ($\Delta\lambda/\lambda = 0.09$). All of the samples produced azimuthally isotropic two-dimensional scattering patterns that were averaged to the one-dimensional form of intensity versus scattering wave vector $|q| = q = 4\pi\lambda^{-1} \sin(\theta/2)$ where θ is the scattering angle. The

TABLE 1: Polymer Molecular Characteristics

sample	$10^2 M_n^a$	ρ (g/cm ³) @ 140 °C	N^b	f_A in block	d_0 (Å)	α ($N_A N_B$) ^{1/2} / N_{AB})
PE- d_8	220	0.897	392			
PEP- d_0	229	0.790	409			
PE- d_6 -PEP- d_0	1083		1925	0.50	464	0.208
PEE- d_2	17.1	0.883 ^b	30.8			
PDMS- d_0	21.7	0.954 ^b	35.0			
PEE- d_2 -PDMS- d_0	127	0.935 ^b	214	0.52	145	0.153
PE- d_6	3.95	0.815 ^c	7.52			
PEO- d_0	5.0	0.989 ^c	7.18			
PE- d_6 -PEO- d_0	21.3	0.973 ^c	32.4	0.45	88	0.227

^a Molecular weights are given on a hydrogen equivalent basis because of the differences in extents of deuteration. ^b Segment volume (v_0) was calculated using $v_0 = 108 \exp[6.85 \times 10^{-4}(T - 25 \text{ °C})]$. See ref 13. Actual densities were measured at RT. ^c Molecular weight, temperature, and deuterium substitution corrected densities at 140 °C.

scattering data were corrected for background and cell scattering, detector sensitivity, sample thickness, and transmission. The SANS data from NIST were converted to an absolute differential scattering cross section per unit sample volume (cm⁻¹) by calibration with an aluminum standard as previously described.²²

Rheology. The samples were thermostated in a controlled nitrogen atmosphere. Dynamical mechanical data were recorded on one of the following instruments depending on the nature of the sample: a Rheometrics Solids analyzer RSA 2 equipped with a shear sandwich geometry, a Rheometrics mechanical spectrometer RMS 800 equipped with a parallel plate geometry, or a Rheometrics fluids spectrometer RFS 8400 equipped with a parallel plate geometry.

Cloud Point Determination. Cloud points for the low-molecular-weight polymer blends were obtained visually using blend samples prepared in ampules as described above. The samples were first blended by heating the ampules in a small oil bath with stirring to give a one-phase mixture. They were then immersed in a thermostated (± 0.1 °C) silicon oil bath equipped with a viewing window (Schott Geräte CT 1150). The temperature of the oil bath was lowered in 5–10 °C increments and equilibrated. At or below the phase-separation temperature the samples became opaque and quickly phase-separated. After the crude phase separation temperature was determined, the samples were reheated and slowly cooled (1 °C increments) to define the phase-separation temperature more precisely.

Results

A complete description of the phase behavior for homopolymer and block copolymer ternary blends will depend on a large set of molecular and thermodynamic variables. To simplify our analysis of the blend systems presented in this paper, we have focused on symmetric systems. The molecular weights of the homopolymer pairs are nearly equal ($N_A \approx N_B = N_H$), the volume fractions of homopolymer A and homopolymer B are equal in the ternary mixtures ($\Phi_A = \Phi_B$) within the accuracy of our density estimates, and the composition of the block copolymers used in this study was approximately symmetric ($f_A \approx 0.5$). Furthermore, by designing all three systems to have a ratio of homopolymer to block copolymer molecular weight ($\alpha \equiv N_H/N_{AB}$) to be approximately 0.2 (see Discussion), we can directly compare the locations of the bicontinuous microemulsion channels. The phase diagrams reduce to plots of T vs the total homopolymer concentration (Φ_H) for a given α .

The three-phase diagrams as a function of homopolymer content and temperature for the chemically distinct systems are shown in Figure 3. (We will refer to the ternary blends for the PE-PEP/PE/PEP, PEE-PDMS/PEE/PDMS, and PE-PEO/PE/PEO systems as the EP, EED, and EO systems, respectively.)

In Figure 3a the phase diagram from the model EP system has been reproduced from our earlier work.¹² There are striking similarities among these three-phase diagrams. On the block-copolymer-rich side, a line of order–disorder transitions (ODTs) was observed in each of the systems (lamellar (L) \rightarrow DIS or hexagonal (H) \rightarrow DIS). On the homopolymer-rich side of the phase diagrams a line of transitions separates one-phase and phase-separated regions. These transitions can be described as critical points or nearly critical points depending on the proximity to perfectly symmetric conditions. Details of the phase-separated region have not been presented in these diagrams. For example, there may be a three-phase window within the phase-separated region; the details of this region are currently being explored. Interesting, nonclassical critical phenomena appear in the one-phase region at temperatures just above the one-phase/phase-separated boundary. This aspect of the mixing thermodynamics is also deferred to other reports. In the EP mixtures we reported the existence of a narrow bicontinuous microemulsion channel separating the lamellar and two phase regimes. In both the EED and the EO mixtures a similar channel of bicontinuous microemulsion was observed. These ternary phase diagrams can be generally divided into the three domains described above: order–disorder, one-phase/phase-separated, and the bicontinuous microemulsion channel. Characterization of the microemulsion channel will be followed by a description of the order–disorder region and finally the one-phase and phase-separated regions.

The dashed lines in each of the diagrams shown in Figure 3 delineate the channel of bicontinuous microemulsion, which we have characterized by small-angle neutron scattering. On the basis of a Landau free energy expansion, Teubner and Strey obtained a static scattering intensity function $I(q)$ for microemulsions,²³

$$I(q) = \frac{\text{constant}}{a_2 + c_1 q^2 + c_2 q^4} \quad (1)$$

where a_2 , c_1 , and c_2 are composition-dependent coefficients and q is the magnitude of the scattering wave vector. In Figure 4 experimental scattering curves for the EO system at $\Phi_H = 0.803$ are given for four representative temperatures. The scattering data from this mixture were fit using eq 1.²⁴ The Teubner–Strey fits at each temperature are rather good, with the exception of the high q data at the two lower temperatures.²⁵ Similar fits were obtained for the EED system at a homopolymer composition $\Phi_H = 0.900$ (Figure 5). The experimental temperature window for the EED system is larger than that for the EO system, which is limited by crystallization of both the PE and the PEO.²⁶ Therefore, SANS data were obtained deep in the

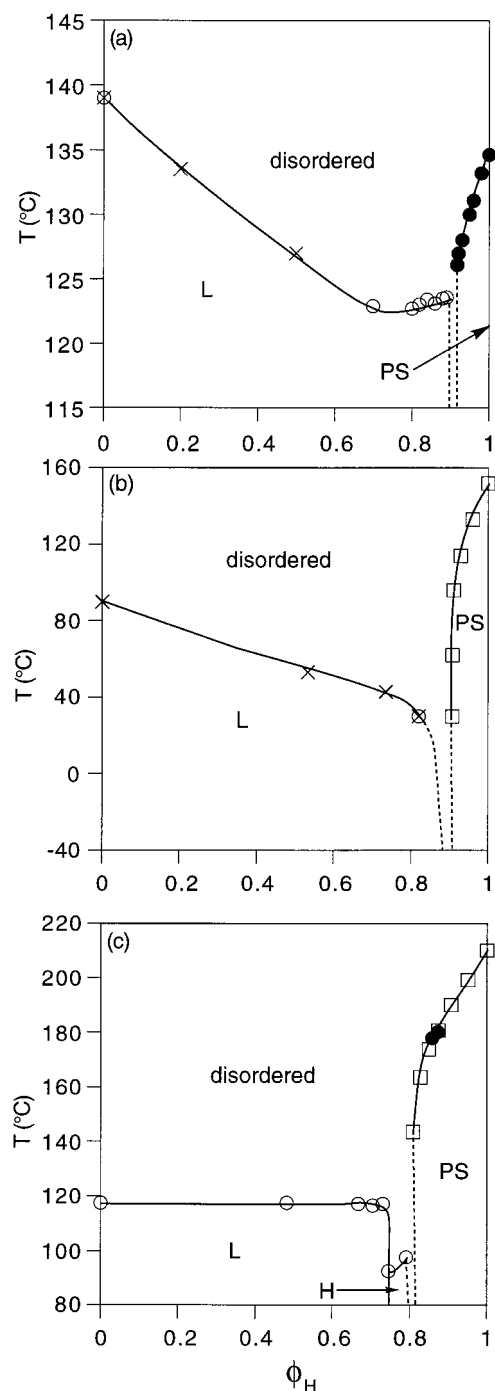


Figure 3. Phase diagrams for the three chemically distinct block copolymer/homopolymer systems: (a) EP; (b) EED; (c) EO (see text for explanation). The phase boundaries depicted were obtained by a variety of techniques: (x) order–disorder transition observed rheologically; (open circles) order–disorder transition observed by SANS; (filled circles) phase separation as determined by SANS; (open squares) phase separation as determined by visual cloud point measurements. Φ_H = concentration of homopolymer in the ternary blend, L = lamellar phase, H = hexagonal phase, PS = phase-separated region. The dashed lines in the phase diagrams delineate the bicontinuous microemulsion channel.

microemulsion channel for the EED system. Figure 5d shows SANS data taken at -39 °C. This channel of bicontinuous microemulsion has a much larger temperature window than typical oil/water/surfactant mixtures.²⁷

Transmission electron microscopy (TEM) is difficult, if not impossible, to use with the relatively low-molecular-weight EED and EO systems. In the EP system we obtained TEM images

of the ternary mixture in the bicontinuous microemulsion channel to verify its existence.¹³ Within the bicontinuous microemulsion channel we have also obtained SANS data and fit the data with eq 1. The SANS data and a TEM image of the bicontinuous microemulsion are shown in Figure 6. The SANS data for the EP system containing 10% block copolymer ($\phi_H = 0.900$) are in good agreement with the Teubner–Strey fit except for $q \geq 2q^*$.²⁵ We have deduced that a channel of microemulsion exists in the EO and EED systems by analogy with the EP results and by virtue of the nearly symmetric nature of these systems (see below).

On the ordering side of the phase diagram the phase boundaries for the EED and EO systems were obtained by rheological measurements or SANS measurements as a function of temperature. A representative example of the ODT determination for an EO mixture containing $\Phi_H = 0.483$ is shown in Figure 7. The sample was heated from 105 to 125 °C in 5 °C intervals with ample equilibration between consecutive temperatures. Well below T_{ODT} (90 °C) the sample exhibits a sharp and intense peak with a higher order reflection at $2q^*$ (Figure 7, inset). As the sample is heated, the peak intensity drops. Between 115 and 120 °C a discontinuous decrease in the peak intensity, a concomitant increase in the peak width, and a loss of the higher order reflection were observed. This behavior is characteristic of the ODT observed in a variety of neat block copolymer samples.¹³ Using similar analyses, we characterized the ODT temperature for eight of the mixtures in the EED and EO systems (Figure 3).

In the EO system, the order–disorder transition temperatures are composition-independent between $\Phi_H = 0$ and $\Phi_H \approx 0.7$ (Figure 3). At higher homopolymer concentrations in the EO phase diagram, two samples exhibited ordered phases with nonlamellar symmetry. The SANS data for an EO sample containing 20.8% block copolymer ($\Phi_H = 0.792$) is shown in Figure 8. Higher order reflections consistent with a hexagonal phase are evident. This composition is very close to the bicontinuous microemulsion composition ($\Phi_H = 0.803$). A comparison of the two scattering patterns at nearly the same temperature is also shown in Figure 8. Approximately 1% difference in composition leads to significant differences in the scattered intensity as a function of q . The $\Phi_H = 0.803$ sample is clearly not ordered.

On the homopolymer-rich (or one-phase/phase-separated) side of the phase diagrams we relied on two methods for the determination of phase boundaries. The first was visual cloud point measurements. Because of the low molecular weights and significant refractive index contrast of both the EO and the EED mixtures, visualization of the phase separation in these mixtures upon cooling was straightforward. In a thermostated (± 0.1 °C) oil bath, well-mixed combinations of homopolymer and block copolymer were heated into the one-phase region and held at high temperature for an ample equilibration time. The samples were then monitored as the temperature of the oil bath was lowered. At the phase boundary the samples coarsened, became cloudy, and ultimately split into two discrete layers over a period of one to several minutes. This behavior was observed in both the EO and the EED mixtures. From these measurements a line of phase-separation transitions was constructed for both systems (Figure 3).²⁸

SANS is a powerful technique for the evaluation of polymer blend thermodynamics and was very useful for examination of our ternary mixtures.²⁹ We examined two of the EO mixtures on the homopolymer-rich side of the phase diagram using SANS. Mean-field theory (MFT) predicts that the inverse of

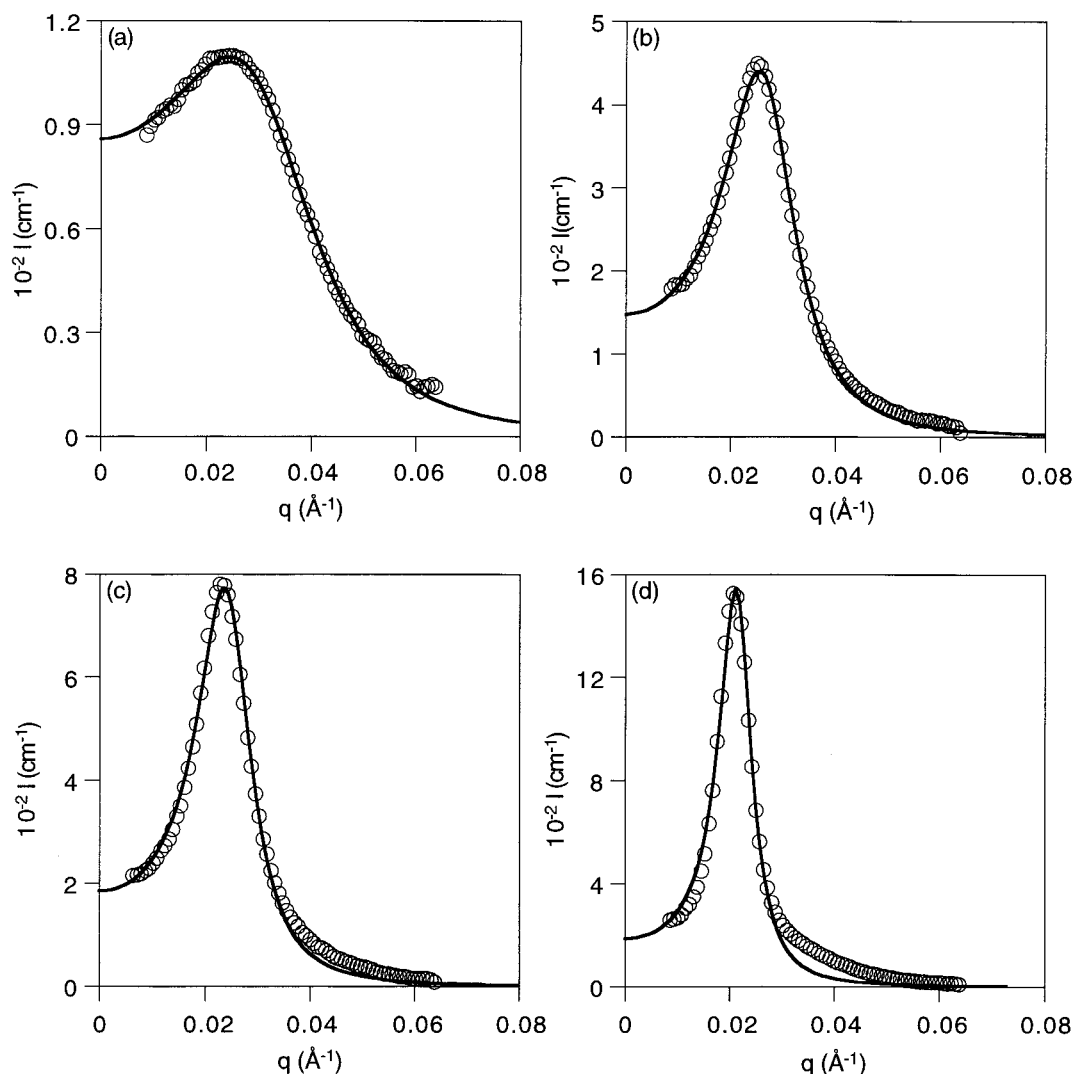


Figure 4. SANS data for the bicontinuous microemulsion channel observed in the EO system at 19.7% block copolymer ($\Phi_H = 0.803$) at (a) 140 °C, (b) 113 °C, (c) 93 °C, and (d) 83 °C. The data were fit using a modified version of eq 1 fitting I_0 , I_{\max} , and q_{\max} simultaneously (see ref 23).

the scattered intensity $I(q)^{-1}$ should scale as q^2 for binary mixtures of homopolymers.²⁹ In block copolymer/homopolymer mixtures, however, we have shown that added block copolymer results in a q^4 component to the scattered intensity, and at a special composition coincident with the Lifshitz composition in the phase diagram $I(q)^{-1}$ is linear in q^4 in the experimental low q limit. The SANS data for an EO mixture containing 14.2% block copolymer ($\Phi_H = 0.858$) are shown in Figure 9 in the Ornstein–Zernike ($c_2 = 0$) format.²⁹ A linear least-squares regression is drawn through each set of data, and the fits are consistent with the Ornstein–Zernike analysis even at the relatively high block copolymer concentration. Any significant contribution from a q^4 component would impart a nonlinear component to this representation. By plotting the scattered intensity at $q = 0$ versus $1/T$ (not shown), we were able to extrapolate to a stability temperature that was about 2 °C lower than the phase-separation temperature; the latter was associated with a distinct departure from Ornstein–Zernike behavior and a steady reduction in $I(q)$ with temperature due to the formation of two phases. This SANS-determined binodal temperature agreed with the value determined visually (see above) within experimental error. Thus, the $\Phi_H = 0.858$ mixture is characterized by a (weakly) first-order phase transition indicating that the three-component EO system is slightly asymmetric.

Discussion

Ternary polymer blends containing homopolymer A, homopolymer B, and block copolymer A–B are useful model systems for fundamental phase behavior studies. We have explored regions of phase space in three chemically distinct systems that have allowed us to access a bicontinuous microemulsion phase in each system. The general features of the phase diagrams described here are similar to those observed in the well-studied oil/water/surfactant mixtures. However, by avoiding the peculiar interactions associated with aqueous dispersions, we have been able to expand the region in phase space over which the bicontinuous microemulsion is stable.

We have focused on a special set of homopolymers and block copolymers that have allowed us to explore two extremes of the ternary phase diagram over a similar temperature window. MFT predicts that the order–disorder transition in a symmetric diblock copolymer occurs at $(\chi N_{AB})_{ODT} = 10.5$ and that phase separation in a binary mixture of homopolymers occurs at $(\chi N_H)_c = 2$, where χ is the Flory–Huggins segment–segment interaction parameter. Assuming that a single function for χ can be used for both the block copolymer and the homopolymer mixtures (see Appendix),³⁰ the overall degree of polymerization for the block copolymer (N) must be about 5 times greater than that for either of the corresponding homopolymers for the block

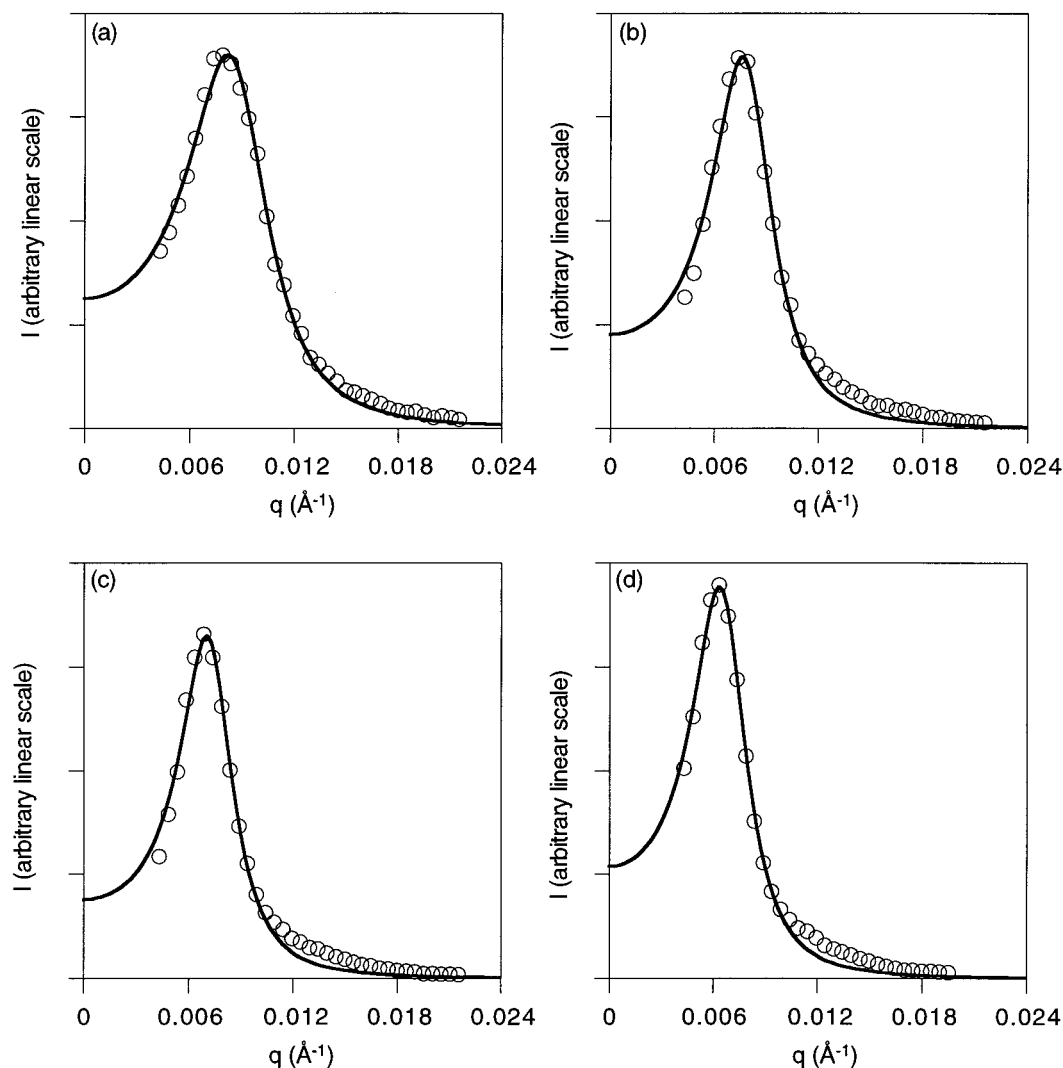


Figure 5. SANS data for the bicontinuous microemulsion channel observed in the EED system at 10.0% block copolymer ($\Phi_H = 0.900$) at (a) 20 °C, (b) 0 °C, (c) -20 °C, and (d) -39 °C. The data were fit using a modified version of eq 1 fitting I_0 , I_{\max} , and q_{\max} simultaneously (see ref 23).

copolymer order-disorder transition temperature to be similar to the homopolymer blend phase-separation temperature. In the three polymeric systems described in this paper, this general criterion has been met. This can be seen in Figure 3 by comparing the ODT temperatures for the pure block copolymers and phase-separation temperatures for the pure homopolymer blends. This design element has allowed us to study a set of blends that contain equal volumes of each of the homopolymers with varying amounts of block copolymer over the same experimental temperature window.

In our previous work on the high-molecular-weight block EP blends, we observed a channel of bicontinuous microemulsion in the region of the phase diagram where MFT predicts an isotropic Lifshitz critical point at $\Phi_{LP} = 1/(1 + 2\alpha^2)$.³¹ This point in the phase diagram is where the lamellar, two-phase, and disordered states meet. An unbinding transition (UT) separates the lamellar and phase-separated regions at temperatures below T_{LP} within the MFT. Adding homopolymer to both sides of the block copolymer interface leads to a swelling of the lamellar phase. The spacing of the lamellar phase increases as the volume fraction of homopolymer increases, and mean-field theory predicts that the spacing will diverge at the UT. (An alternative prediction from MFT suggests that the swollen lamellar phase may separate into two coexisting asymmetric lamellar phases, each rich in either A or B.^{32b}) However, we

have reported that the UT is preempted by the formation of a bicontinuous microemulsion phase. Presumably, this is due to the susceptibility of the system to lamellar fluctuations. This effect was observed in all three systems that vary in molecular weight by nearly 2 orders of magnitude (see Table 1). In all three systems a bicontinuous microemulsion channel separates L (or H) and phase-separated regions of the generic isopleth shown in Figure 1c.

For both the EO and the EED ternary blends we observed the expected lamellar to disorder transitions on the block-copolymer-rich side of the phase diagram, consistent with the EP system. On the ordering side of the EO system, however, we observed what we believe is a hexagonally packed cylindrical phase close to the bicontinuous microemulsion channel. In a theoretical description of the ternary phase triangle for similar block copolymer/homopolymer blends at fixed temperature, a slight asymmetry in either the block copolymer or the ratios of N_A/N_{AB} and N_B/N_{AB} can have a dramatic effect on the symmetry of the phase diagram. For example, according to Janert and Schick,³² a hexagonal phase separates the lamellar and the two phase windows with just a slightly asymmetric block copolymer ($f_A = 0.54$). Although we prepared all three systems to be as symmetric as possible, there is likely to be some degree of asymmetry. For example, differences in molecular weight, along with excess volumes of mixing, could break the assumption of

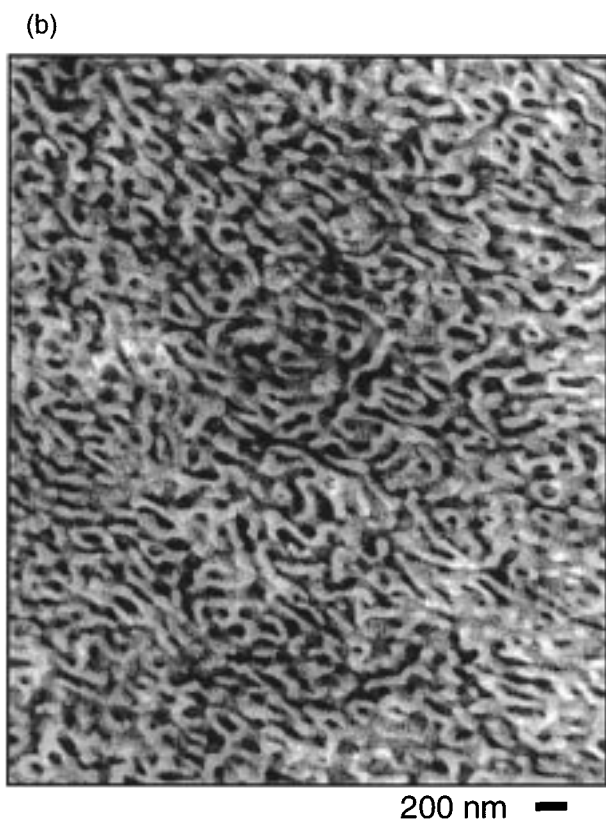
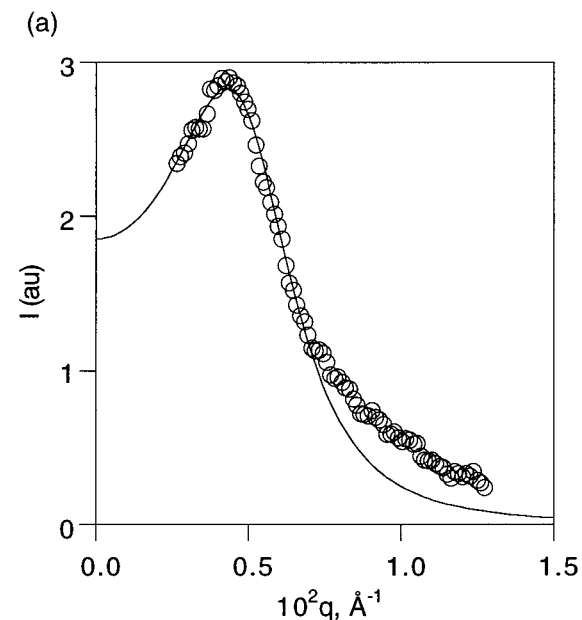


Figure 6. (a) SANS data for the bicontinuous microemulsion channel observed in the EP system at 10.0% block copolymer ($\Phi_H = 0.900$) at 125 °C. The data were fit using a modified version of eq 1 fitting I_0 , I_{\max} , and q_{\max} simultaneously (see ref 23). Only the $q < 0.0074 \text{ \AA}^{-1}$ data were included in the fit (see ref 25). (b) Transmission electron micrograph for the same sample after annealing at 119 °C for 30 min followed by a rapid quench below the crystallization temperature. The PEP components were stained using ruthenium tetroxide and appear dark in the image.

perfect symmetry at $f = 0.5$ and $\Phi_A = \Phi_B = 0.5$.³³ Moreover, unlike the EP system, the intermolecular interactions characterizing the EO system are not purely dispersive, and asymmetry in these interactions may also result in a deviation from the assumed symmetry conditions. The MFT used to describe these ternary mixtures are generally based on a one-parameter

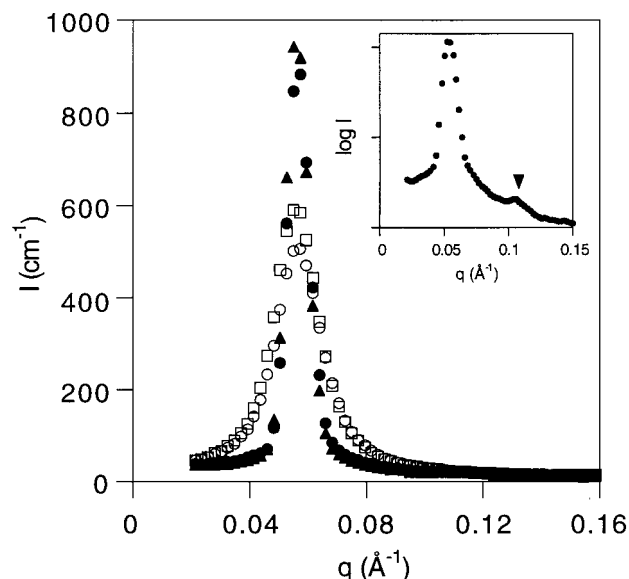


Figure 7. SANS data showing the lamellar order-disorder transition for an EO sample containing 51.7% block copolymer ($\Phi_H = 0.483$): (filled triangles) 110 °C; (filled circles) 115 °C; (open squares) 120 °C; (open circles) 125 °C. The inset shows the ordered state at 90 °C with the higher order reflection clearly present (the triangle is at $2q^*$).

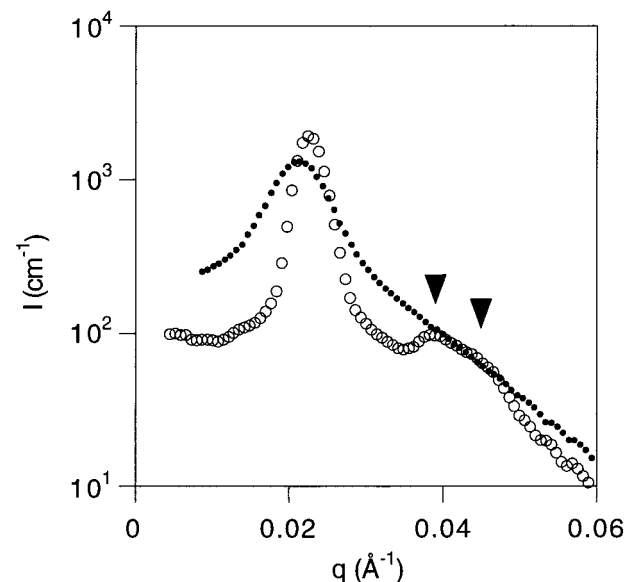


Figure 8. SANS data for an ordered EO mixture containing 20.8% block copolymer ($\Phi_H = 0.792$) at 85 °C (open circles). The triangles are at $3^{1/2}q^*$ and $4^{1/2}q^*$. SANS data for the sample containing 19.7% block copolymer ($\Phi_H = 0.803$) at 83 °C (filled circles, same data as in Figure 4d).

segment-segment interaction parameter between unlike monomers as described by

$$\chi = \frac{z}{kT} \left[\epsilon_{AB} - \frac{1}{2}(\epsilon_{AA} + \epsilon_{BB}) \right] \quad (2)$$

where ϵ_{AB} represents the contact energy between A and B segments, z is the number of segment-segment contacts, and k is the Boltzmann constant. This equation assumes the interaction energy of an A monomer surrounded by B monomers is the same as a B monomer surrounded by A monomers. In the case of polyolefins (e.g., the EP system) this is probably a good assumption. In the EO system this assumption is more tenuous because of the polar nature of PEO relative to PE, and therefore, specific interactions may play a role in the interaction strengths.

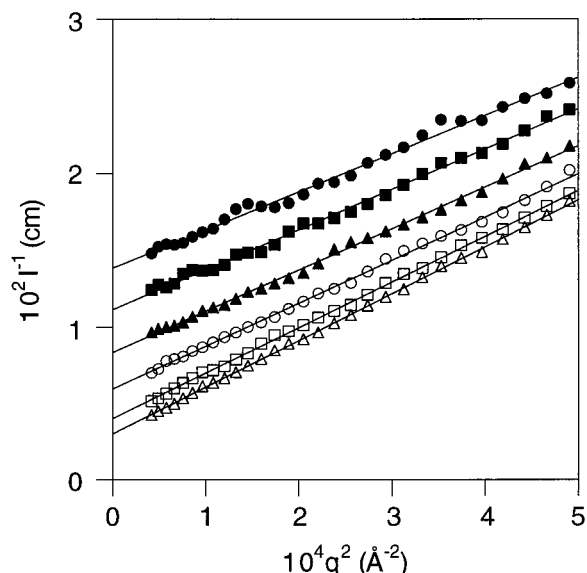


Figure 9. SANS Ornstein–Zernike plot for the EO mixture containing 14.2% block copolymer ($\Phi_H = 0.858$) at (filled circles) 183 °C, (filled squares) 182 °C, (filled triangles) 181 °C, (open circles) 180 °C, (open squares) 179 °C, and (open triangles) 178 °C. At 177 °C phase separation was observed.

Observation of a hexagonal phase at $\phi_H = 0.732$ and $\phi_H = 0.745$ and the (weak) first-order character of the phase-separation point at $\phi_H = 0.858$ both support the notion that the EO isopleth is slightly off symmetry. Conformational mismatches between PE and PEO may also be important in determining the symmetry of the ordered state.³⁴

We relied on cloud point measurements for determining the one-phase/phase-separated boundary on the homopolymer-rich side of the phase diagrams. SANS analysis of one of the homopolymer-rich EO mixtures was informative. We found that the inverse of the scattered intensity was a linear function of q^2 in a mixture containing 14.2% block copolymer ($\Phi_H = 0.858$). In the EP system we found that the binary blend ($\Phi_H = 1$) produced Ornstein–Zernike scattering, but it was necessary to include both q^2 and q^4 terms to model the blend containing $\Phi_H = 0.96$. No q^4 component was necessary in the analysis of the scattering observed in the EO system at $\Phi_H = 0.858$. We are puzzled by this result, which suggests there are some quantitative differences in the critical behavior of low- and high-molecular-weight ternary systems near the putative Lifshitz point. However, owing to the differences in polymer coil dimensions, the scattering measurements were performed at values of qR_g that differ by almost an order of magnitude, and thus, we are not able to make a quantitative comparison.

From the data we gathered on these three systems, we come to the general conclusion that the phase behavior observed in high-molecular-weight polyolefin ternary mixtures is essentially reproduced in the two low-molecular-weight mixtures. The position of the microemulsion channel is located coincident with the predicted Lifshitz point in the EP system. In the EED and the EO systems the location of the bicontinuous microemulsion channel is shifted to lower concentrations of homopolymer than the Lifshitz composition predicted by MFT based on the exact value of α for each of the systems (see Table 1). The difference between the composition of the observed bicontinuous microemulsion channel and the predicted Lifshitz composition ($\phi_{\mu E} - \phi_{LP}$) is approximately 0, 0.06, and 0.11 for the EP, EED, and EO systems, respectively. In an alternative approach to compare the three systems in a universal manner, we plot the principal spacings of the mixtures reduced by the principal

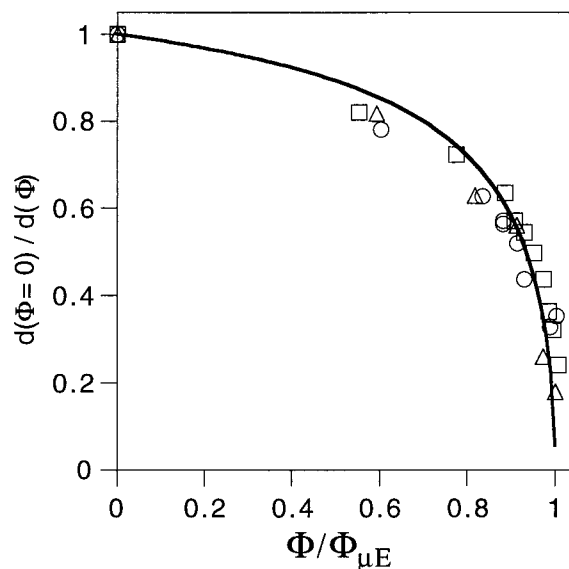


Figure 10. Reduced spacing vs reduced composition for all three ternary mixtures: (circles) EO; (triangles) EED; (squares) EP. The spacings for the EP system were obtained around the order–disorder transition, the spacings for the EED system were obtained around 30 °C, and the spacings for the EO system were obtained around 110 °C. The solid line is the mean-field theory prediction ($\alpha = 0.208$, $\Phi_{\mu E} = 0.920$).³¹

spacing of the component block copolymer, d_0 (determined by SANS) as a function of the mixture composition, reduced by the experimentally determined composition of the bicontinuous microemulsion channel. This is given in Figure 10. All of the data essentially fall on the same curve. In addition, the data are well represented by the mean-field-predicted lamellar spacing dependence with ϕ_H (for $\alpha = 0.208$).³¹ The data given in Figure 10 strongly indicate a universal behavior, but there is currently no theoretical justification for the data reduction scheme.

The existence of the bicontinuous microemulsion phase in each of the chemically distinct systems demonstrates that the original phase behavior observed in the high-molecular-weight polyolefin system (EP) is retained as the molecular weight is reduced. Observation of bicontinuous microemulsion channel is therefore not the consequence of the polymeric nature of the components. The EO system contains molecules that range from a few hundred molecular weight to a few thousand. These molecules are oligomeric and are more closely related to the small molecules typical of surfactant systems. This feature allows the investigation of polymer thermodynamics using relatively small molecules where the system is not kinetically hindered and can readily equilibrate. The EO system is ideal not only in this sense but also because water can be introduced thereby bridging polymeric and conventional surfactancy in a systematic manner.

Acknowledgment. This work was supported by the National Science Foundation (NSF/DMR-9405101) and the Center for Interfacial Engineering, an Engineering Research Center at the University of Minnesota, and in part by the MRSEC program of the National Science Foundation under Award No. DMR-9809364. We thank Mark W. Hamersky (UM) and Charles J. Glinka (NIST) for technical assistance with the SANS data acquisition. We are also grateful for cloud point measurements and helpful comments provided by Terry Morkved and Petr Stepanek.

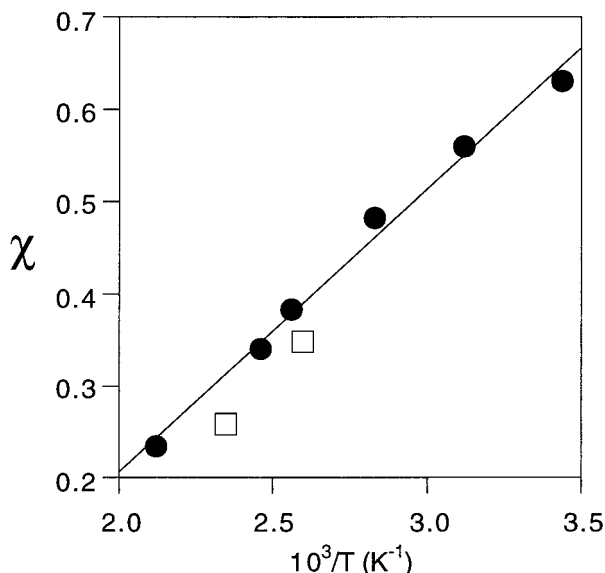


Figure 11. Interaction parameter χ as a function of inverse temperature for a series of alkane/PEO binary blends (filled circles) and two PE-PEO block copolymers (open squares).

Appendix

One of the most common assumptions in dealing with polymer blend and block copolymer phase behavior is that the universal mean-field description is appropriate. In symmetric binary polymer blends ($N_A = N_B = N$) the mean-field critical condition is given by $(\chi N)_c = 2$, whereas for symmetric diblock copolymers $(\chi N)_{ODT} = 10.5$. Although there are well-established fluctuation corrections to both classes of phase behavior,³⁵ the magnitudes of these effects at high molecular weight are generally quite small. In a recent study³⁰ we showed that the order-disorder transition temperature (T_{ODT}) for PE-PEP diblock copolymers ($88\,000 \leq M_n \leq 128\,000$ g/mol) could be closely (although not precisely) anticipated based on a $\chi(T)$ determination from a PE/PEP homopolymer blend using mean-field analysis and assuming $(\chi N)_{ODT} = 10.5$. An important question germane to the study presented in this article is whether these mean-field concepts remain viable with our lowest molecular weight EO system, which has just $1/60$ the degree of polymerization of the EP system (see Table 1).

We have evaluated the thermodynamic correspondence between PEO and PE in homopolymer and diblock forms using the strategy described in ref 30. Six oligomeric blends of PE and PEO, containing 50 vol % of each component, were sealed in glass ampules and equilibrated at a series of temperatures using an oil bath. Upper consolute temperatures were clearly evidenced by a transition from two phases to one upon heating and vice versa with cooling. Four linear alkanes (C15, C16, C20, and C32) and five relatively monodisperse ($M_w/M_n \approx 1.2$) PEO specimens (Fluka, $M_n = 178, 222, 250, 400$, and 500 , g/mol) were combined as follows: C15/178, C15/222, C16/250, C16/400, C20/400, and C32/500. The blend degree of polymerization was approximated as $N = (N_{PEO}N_{PE})^{1/2}$ where N_{PEO} and N_{PE} refer to the weight average number of 126 \AA^3 volume elements (i.e., segments) per molecule at $140 \text{ }^\circ\text{C}$. These calculations made use of the (molecular weight dependent) density of each component. Although none of the six mixtures is perfectly symmetric, the effects of slightly mismatched N 's on our estimation of $\chi(T)$ are not very significant. The χ values were assigned to each phase-transition temperature by assuming $\chi N = 2$. Anticipating the conventional temperature dependence $\chi = AT^{-1} + B$, we have plotted χ versus T^{-1} in Figure 11.

These data points are well represented by $\chi = 0.361T^{-1} - 0.589$.

ODT temperatures were determined for two nearly symmetric PEO-PE diblock copolymers using dynamic mechanical spectroscopy measurements as described elsewhere.^{18b} The results were $T_{ODT} = 112 \text{ }^\circ\text{C}$ for $M_n = 2130$ g/mol (this polymer is identified in Table 1) and $T_{ODT} = 153 \text{ }^\circ\text{C}$ for $M_n = 2800$. $N = N_{PE} + N_{PEO}$, in this case the number average value, was calculated using the same functions established for the (molecular weight dependent) densities of the corresponding homopolymers and a segment volume of 126 \AA^3 . Finally, χ was calculated assuming $(\chi N)_{ODT} = 10.5$. The results are also plotted in Figure 11.

Remarkably, this crude analysis produced agreement between the binary blend and diblock copolymer χ values that rivals the results reported for the much higher molecular weight EP system. (Note that in the previous study an in-depth analysis of fluctuation effects was also included.) A more comprehensive treatment of these results lies outside the scope of the present discussion. Nevertheless, the results summarized in Figure 11 provide strong support for our hypothesis that the ternary mixtures can be quantitatively compared notwithstanding the large disparity in molecular weights. Moreover, it further suggests that unentangled low-molecular-weight mixtures, which equilibrate quickly, are appropriate systems for studying the thermodynamic and dynamic processes in the vicinity of the bicontinuous microemulsion channel.

References and Notes

- (1) Kahlweit, M. *Science* **1988**, *240*, 617-621.
- (2) Jahn, W.; Strey, R. *J. Chem. Phys.* **1988**, *92*, 2294.
- (3) Gelbart, W. M.; Benschaul, A. *J. Phys. Chem.* **1996**, *100*, 13169-13189.
- (4) (a) *Micelles, Membranes, Microemulsions, and Monolayers*; Gelbart, W. M., Ben-Shaul, A., Roux, D., Eds.; Springer: New York, 1994. (b) Gompper, G.; Schick, M. *Self-Assembling Amphiphilic Systems*; Academic Press: London, 1994.
- (5) (a) Antonietti, M.; Hentze, H. P. *Colloid Polym. Sci.* **1996**, *274*, 696-702. (b) Antonietti, M.; Hentze, H. P. *Adv. Mater.* **1996**, *8*, 840-844.
- (6) Schwuger, M.-J.; Stickdorn, K.; Schomäcker, R. *Chem. Rev.* **1995**, *95*, 849-864.
- (7) For examples, see the following. (a) Talmon, Y.; Prager, S. *J. Chem. Phys.* **1978**, *69*, 2984-2991. (b) Kahlweit, M.; Strey, R. *Angew. Chem., Int. Ed. Engl.* **1985**, *24*, 654-668. (c) Andelman, D.; Cates, M. E.; Roux, D.; Safran, S. A. *J. Chem. Phys.* **1987**, *87*, 7229. (d) Kahlweit, M.; Strey, R.; Busse, G. *J. Phys. Chem.* **1990**, *94*, 3881-3894. (e) Mallamace, F.; Micali, N.; Chen, S. H. *J. Appl. Crystallogr.* **1997**, *30*, 1105-1111.
- (8) (a) Hecht, E.; Mortensen, K.; Hoffman, H. *Macromolecules* **1995**, *28*, 5465-5476. (b) Strey, R.; Schomäcker, R.; Roux, D.; Nallet, F.; Olsson, U. *J. Chem. Soc., Faraday Trans.* **1990**, *86*, 2253-2261.
- (9) Kahlweit, M.; Strey, R.; Haase, D.; Firman, P. *Langmuir* **1988**, *4*, 785-790.
- (10) For example, see the following. Macosko, C. W.; Guegan, P.; Khandpur, A. K.; Nakayama, A.; Marechal, P.; Inoue, T. *Macromolecules* **1996**, *29*, 5590-5598.
- (11) Bates, F. S.; Maurer, W. W.; Lodge, T. P.; Schulz, M. F.; Matsen, M. W.; Almdal, K.; Mortensen, K. *Phys. Rev. Lett.* **1995**, *75*, 4429-4432.
- (12) Bates, F. S.; Maurer, W. W.; Lipic, P. M.; Hillmyer, M. A.; Almdal, K.; Mortensen, K.; Fredrickson, G. H.; Lodge, T. P. *Phys. Rev. Lett.* **1997**, *79*, 849.
- (13) Rosedale, J. H.; Bates, F. S.; Almdal, K.; Mortensen, K.; Wignall, G. D. *Macromolecules* **1995**, *28*, 1429-1443.
- (14) Morkved, T. L.; Chapman, B. R.; Bates, F. S.; Lodge, T. P.; Stepanek, P.; Almdal, K. *Faraday Discuss.*, in press.
- (15) The phenomenological connection between the phase behavior observed in surfactant systems and block copolymer melts has been made by us and others. See the following. (a) Bates, F. S.; Schulz, M. F.; Khandpur, A. K.; Förster, S.; Rosedale, J. H. *Faraday Discuss.* **1994**, *98*, 7-18. (b) Gruner, S. M. *J. Phys. Chem.* **1989**, *93*, 7562-7570.
- (16) Hillmyer, M. A.; Bates, F. S. *Macromolecules* **1996**, *29*, 6994.
- (17) (a) Hillmyer, M. A.; Bates, F. S.; Ryan, A. J.; Almdal, K.; Mortensen, K.; Fairclough, J. P. *Science* **1996**, *271*, 976. (b) Hajduk, D. A.; Kossuth, M. B.; Hillmyer, M. A.; Bates, F. S. *J. Phys. Chem. B* **1998**, *102*, 4269.

- (18) (a) Almdal, K.; Mortensen, K.; Ryan, A. J.; Bates, F. S. *Macromolecules* **1996**, *29*, 5940–5947. (b) Almdal, K.; Hillmyer, M. A.; Bates, F. S. *Macromolecules*, in press.
- (19) Fetters, L. J.; Lohse, D. J.; Richter, D.; Witten, T. A.; Zirkel, A. *Macromolecules* **1994**, *27*, 4639–4647.
- (20) *Physical Properties of Polymers Handbook*; Mark, J. E., Ed.; American Institute of Physics: Woodbury, NY, 1996.
- (21) The volume fraction of PEO in EO-1 using the corrected densities of the component blocks is different from the densities reported in ref 15, since the high-molecular-weight densities were used in that reference.
- (22) Wignall, G. D.; Bates, F. S. *J. Appl. Crystallogr.* **1987**, *20*, 28.
- (23) Teubner, M.; Strey, R. *J. Chem. Phys.* **1987**, *87*, 3195–3199.
- (24) Equation 1 can be rewritten in terms of the scattered intensity I_{\max} at $q = q_{\max}$, I_0 at $q = q_0$, and the wave vector q_{\max} . All three variables were fit simultaneously.
- (25) In all of the Teubner–Strey fits the high q ($qR_g > 1$) data are always above the predicted fit. At high q the $I(q)$ data are predicted to scale as q^{-4} for a microemulsion as described by Teubner and Strey. We attribute this intensity to chain scattering from within the large-scale domain structure of the microemulsion. This will produce scattering that scales as q^{-2} (Gaussian coil scattering). For the EO and EED microemulsion data we fit the entire data set to eq 1. For the EP data, however, we fit the low- q data only (peak). For a discussion of the scaling at large q for Gaussian chains, see Chapter 6 in ref 28.
- (26) The PE in both the block copolymer and the binary blends limits the lower temperature that can be accessed experimentally. For the block copolymer this temperature is 90 °C, and for the binary blend 60 °C is the low-temperature limit.
- (27) In alkylpolyglucoside-based surfactant systems the temperature stability of microemulsions can be increased relative to typical nonionic surfactants (ethyleneoxide-based); however, stability ranges of only 20 °C are considered large in these systems. Fukuda, K.; Söderman, O.; Lindman, B.; Shinoda, K. *Langmuir* **1993**, *9*, 2921–2925.
- (28) Two of the cloud point measurements in the EED phase diagram ($\phi_H = 0.908$) were obtained by monitoring the transmitted intensity via laser light scattering experiments.
- (29) Higgins, J. S.; Benoît, H. C. *Polymers and Neutron Scattering*; Oxford University Press: New York, 1994.
- (30) Maurer, W. W.; Bates, F. S.; Lodge, T. P.; Almdal, K.; Mortensen, K.; Fredrickson, G. H. *J. Chem. Phys.* **1998**, *108*, 2989–3000.
- (31) Broseta, D.; Fredrickson, G. H. *J. Chem. Phys.* **1990**, *93*, 2927–2938.
- (32) (a) Janert, P. K.; Schick, M. *Macromolecules* **1997**, *30*, 137–144. (b) Janert, P. K.; Schick, M. *Macromolecules* **1997**, *30*, 3916–3920.
- (33) All of the densities for the EO system were calculated, and there may be systematic error in the ratio of homopolymer concentrations (Φ_A/Φ_B) that could also lead to a departure from the lamellar phase.
- (34) Matsen, M. W.; Schick, M. *Macromolecules* **1994**, *27*, 4014–4015.
- (35) For block copolymers see the following. Fredrickson, G. H.; Helfand, E. *J. Chem. Phys.* **1987**, *87*, 697. For homopolymers see the following. Schwahn, D.; Meier, G.; Mortensen, K.; Janssen, S. *J. Phys. II (France)* **1994**, *4*, 837.